Si-H and N-H vibrational properties in glow-discharge amorphous SiNx:H films (0<x<1.55)

Si-H and N-H vibrational properties in glow-discharge amorphous SiN_x:H films ($0<x<1.55$)

Seiichi Hasegawa, Masaaki Matsuda, and Yoshihiro Kurata
Department of Electronics, Faculty of Technology, Kanazawa University, Kanazawa 920, Japan

(Received 11 June 1990; accepted for publication 27 August 1990)

Amorphous SiN_x:H films were prepared by rf glow discharge of SiH_4-NH_3 mixtures at 300 °C, and the SiH, NH, and SiN vibrational absorptions were investigated as a function of x. The stretching absorption profiles due to SiH and SiN bonds are reproduced by a superposition of two components at around 2000 and 2100 cm^{-1}, and of three components at around 750, 840, and 960 cm^{-1}, respectively. The dependence of these intensities on x was examined by means of a generation probability analysis on the basis of the random bonding model including SiH and NH bonds which play an important role in the film growth mechanism.

Glow-discharge amorphous (GD a-) SiN_x:H films have attracted growing interest because of their potential for wide applications in microelectronics, as an insulator in thin-film transistors[1-3] and passivation layers.[4] N atoms incorporated into the host Si network are bonded to three Si atoms at a relatively low N content (x in SiN_x),[5,6] and N atoms with two Si atoms and one H atom as nearest neighbors occur at a higher x.[7,8] In recent papers,[9,10] we have investigated the vibrational properties of SiH and SiN bonds in GD a-SiN_x:H films prepared from a SiH_4-N_2-H_2 mixture, and shown that the profiles of the SiH stretching absorption are reproduced by a superposition of two components with Gaussian shapes at around 2000 and 2100 cm^{-1}, and that the stretching absorption due to SiN bonds is divided into three components at around 750, 840, and 960 cm^{-1}. In this letter, we examine the dependence of the SiH, NH, and SiN absorption intensities on x for GD a-SiN_x:H films prepared from a SiH_4-NH_3 mixture, by means of a generation probability analysis on the basis of the random bonding model.

The samples were deposited onto fused quartz substrate by GD decomposition of a feed gas in an inductively coupled reactor inserted into an electric furnace set at 300 °C. The details of the fabrication system have been described elsewhere.[11] The gas volume ratio NH_3/SiH_4 was varied from 0 to 30. The total flow rate and pressure were maintained at 10 sccm and 0.3 Torr, respectively, and the rf power was 10 W. The N content x in SiN_x was estimated by means of electron probe microanalysis (EPMA). The densities of SiH and NH bonds were estimated from the intensities of SiH and NH stretching absorption, using the oscillator strength of 1.4×10^{20} (Ref. 12) and 2.8×10^{20} cm^{-2} (Ref. 13), respectively.

Figure 1(a) shows the ratio SiH/Si of the SiH density for the 2000 and 2100 cm^{-1} bands to that of host Si atoms, and Fig. 1(b) shows the ratio SiH/Si for the sum of both SiH bands and the NH/Si ratio, as a function of the observed x (= N/Si). The SiH/Si ratio for the 2000 cm^{-1} band monotonically decreases with x, and disappeared at around $x = 1.0$. This band is assigned to isolated SiH bonds without nearest neighbor N atoms. By contrast, the SiH/Si ratio for the 2100 cm^{-1} band increases with x up to $x = 0.5$, keeping a fixed peak wave number of 2100 cm^{-1}. We have proposed that this band is due to increased formation of N—SiH bonds.[9,10] Above $x = 0.5$, this band rapidly decreased with x, and the peak wave number shifted toward higher wave number. This has been interpreted as indicating further replacement by N atoms of the H and Si nearest neighbors at a Si site in N—SiH bonds.[9,10] As shown in Fig. 1(b), the NH/Si ratio increases with x up to $x = 1.0$, and then is saturated. Above $x = 0.7$, the NH/Si ratio becomes higher than the SiH/Si ratio. Similar results have also been observed for a-SiN_x:H films from a

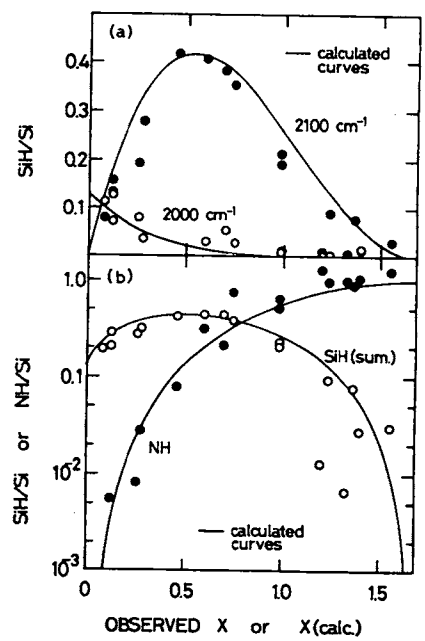

FIG. 1. (a) Ratios SiH/Si of the density of SiH bonds to that of host Si atoms for the 2000 cm^{-1} (○) and 2100 cm^{-1} (●) bands, and (b) the ratio SiH/Si (○) for the sum of both bands in (a) and the ratio NH/Si (●), as a function of the observed N content x determined by EPMA. The solid curves as a function of x(calc) are calculated by the random bonding model including SiH and NH bonds.

Reprinted from Appl. Phys. Lett., Vol.57,No.21,pp.2211~2213 (1990.11)

TABLE I. Random bonding model including SiH and NH bonds for a-SiN_x:H.

n	Standard configurations	N/Si (x_n^*)	$f_p(n)$	Configurations including H	N/Si (x_n^*)	SiH/Si x_n(SiH)	NH/Si x_n(NH)
0	$Si(Si_4)$	0	$(1-px)^4$	H-$Si(Si_3)$	0	1	0
1	$Si(Si_3N)$	1/3	$4(px)(1-px)^3$	H-$Si(Si_2N)$	2/6	1	0
2	$Si(Si_2N_2)$	2/3	$6(px)^2(1-px)^2$	H-$Si(SiN_2)$	4/6	1	0
3	$Si(SiN_3)$	3/3	$4(px)^3(1-px)$	HN-$Si(SiN_2)$	7/6	0	1/2
4	$Si(N_4)$	4/3	$(px)^4$	$(HN)_2$-$Si(N_2)$	10/6	0	1

SiH_4 -N_2-H_2 mixture; the SiH density took the maximum at $x = 0.5$–0.6 (Refs. 9 and 10), and above $x = 0.7$ a higher density of NH bonds than SiH bonds was observed. Thus, the densities of SiH and NH bonds strongly depend on the value of x independent of the preparation conditions.

How can the dependences of the SiH and NH densities in connection with x be explained? By the random bonding model in SiN_x proposed by Knolle and Osenbach[14] the probability that a N atom will be bonded to a Si atom is given by px. Also the probability that a Si atom bonds to a Si atom is $(1-px)$. In a stoichiometric Si_3N_4 film, the probability must satisfy the relation $(p4/3)^4 = 1$, therefore $p = 0.75$. Here, it is assumed that the N atom takes the threefold coordination and N—N bonds are absent as proposed by some research groups.[5,6] H atoms were also excluded from the estimation. In the second column of Table I, we show five possible configurations corresponding to the number, n, of N atoms bonded to a Si atom. The third and fourth columns, respectively, give the N/Si ratio x_n^* in a unit cell and the probability $f_p(n)$ occurring for each configuration for a given x. Now we introduce hydrogen to form SiH and NH bonds into five standard configurations. The SiH bonds will be introduced by replacing one Si nearest neighbor in $Si(Si_{4-n}N_n)$ by a H atom. Here, we neglect the formation of SiH_2 or SiH_3 bonds, because the SiH absorption in a-Si:H films mainly arise from the 2000 cm^{-1} band due to isolated SiH bonds, and the observed fixed peak wave number (2100 cm^{-1}) in a-SiN_x:H films with x below 0.5 is considerably smaller than that predicted for N-SiH_2 or N-SiH_3 (Ref. 15). Therefore, the 2000 and 2100 cm^{-1} bands, respectively, will be due to H-$Si(Si_3)$ and H-$Si(SiN_n)$, as proposed in the previous paper.[9,10]

As shown in Fig. 1, above $x = 0.7$ the NH density becomes higher than the SiH. The value of $x = 0.7$ means that a Si atom is bonded to about two N atoms on the average, because a weighted average number of N atoms bonded to a Si atom in the SiN_x is given by $3x$, excluding H. Accordingly, we assume that at $n > 3$ the Si nearest neighbors at the Si site in $Si(Si_2N_2)$ bonds are replaced by NH with increasing x. Here, we discuss a reason for the generation of NH bonds at $n > 3$. According to the local bonding at the Si and N sites in Si_3N_4, a Si atom with four N nearest neighbors takes a tetrahedral structure, and a N atom with three Si neighbors is in the center of an equilateral triangle of the Si atoms.[16] In the case of GD a-SiN_x:H films, when n is 2, the distance between two Si atoms bonded to each of two N nearest neighbors at a Si site may become too short in part of the bonding network, because of the bonding irregularity. Occurrence of such a bonding geometry will be highly frequent at $n > 3$. This bonding geometry, however, should be unstable because of the occurrence of a high compressive stress, therefore $HN(Si_2)$ bonds are expected to be formed instead of $N(Si_3)$ bonds to relax the stress. Figure 2 shows a schematic representation of the local bonding geometry for (a) the five standard configurations and (b) the corresponding five configurations including SiH and NH bonds. Also in the fifth column of Table I, the five configurations with H are summarized, and the sixth to eighth columns, respectively, give the N/Si $[= x_n^*]$, SiH/Si $[= x_n\ (\mathrm{SiH})]$, and NH/Si $[= x_n\ (\mathrm{NH})]$, ratios in a unit cell.

In each standard configuration occurring at a probability $f_p\ (n)$, if a portion of it [the ratio $A_p\ (n)$] is replaced by the corresponding configuration with H, we can estimate the ratios, SiH/Si and NH/Si, i.e., the ratio of the densities of SiH and NH bonds to the density of Si in a film for a given x as follows:

$$\mathrm{SiH/Si} = A_p(0)x_0(\mathrm{SiH})f_p(0) + \sum_{n=1}^{2} A_p(n)x_n(\mathrm{SiH})f_p(n), \quad (1)$$

$$\mathrm{NH/Si} = \sum_{n=3}^{4} A_p(n)x_n(\mathrm{NH})f_p(n). \quad (2)$$

Here, as revealed in Table I and Fig. 2, the first term in Eq. (1) gives the density of SiH bonds without N nearest neighbors and gives the 2000 cm^{-1} band, and the second term gives those with one or two N atom neighbors responsible for the 2100 cm^{-1} band. Furthermore, the value of x expected to be actually observed for films with H can be estimated by

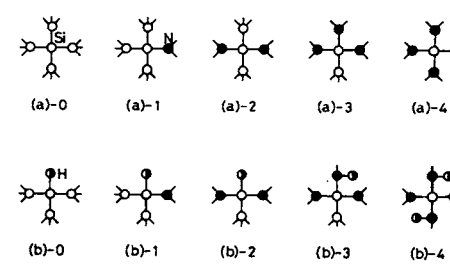

FIG. 2. Schematic representation of the local bonding geometry near a Si—N bond. (a) The five standard configurations without hydrogen, and (b) the corresponding five configurations including SiH and NH bonds.

$$x(\text{calc}) = \sum_{n=1}^{4} \{[1 - A_p(n)]x_n^* f_p(n) + A_p(n)x_n^* f_p(n)\}. \quad (3)$$

From Eqs. (1)–(3), by selecting the proper $A_p(n)$ values, the values of SiH/Si, NH/Si, and x(calc) are calculated as a function of the parameter x determining f_p (n) (see Table I). Accordingly, we can obtain the calculated values of SiH/Si and NH/Si as a function of x(calc). The results are compared with the observed SiH/Si and NH/Si ratios as a function of the observed x, and are represented by the solid curves in Figs. 1(a) and 1(b). Here, we selected $A_p(0) = 0.13$, $A_p(1) = 0.55$, A_p $(2) = 0.65$, and A_p (3 and 4) = 1.0. The observed values of SiH/Si and NH/Si are found to fit well to each calculated curve, indicating the applicability of the random bonding model using SiH and NH bonds. Also the increase in $A_p(n)$ with increasing n indicates that the formation of SiH and NH bonds plays an important role in the film growth mechanism, probably in order to reduce the stress as stated above.

By the random bonding model including NH bonds, the dependence of the SiN absorption on x can also be explained. The main absorption for the SiN asymmetric stretching mode was observed at around 840 and 960 cm^{-1}. Similar absorptions have also been observed for films prepared from a SiH_4-N_2-H_2 mixture,[10] and the 840 and 960 cm^{-1} bands were assigned to N—SiH and Si—N·SiN_n (or N—Si·SiN_n) bonds for the former, and to N_n—Si ($n \geq 2$) bonds for the latter. Della Sala *et al.*[17] also assigned the 840 and 970 cm^{-1} bands to N-Si(Si_3) and N-Si(N_3), respectively. Figure 3 shows the integrated absorption intensity for the 840 and 960 cm^{-1} bands. In the 960 cm^{-1} band, the intensity rapidly increases with x after the absorption begins at around $x = 0.4$. This result cannot be explained fully by the above assignments, but the dependence is similar to that of the density of NH bonds shown in Fig. 1. Therefore, we assume that the 960 and 840 cm^{-1} bands arise from Si—NH—Si and Si—N(Si_2) bonds, respectively. Another reason supporting this assumption, the Si—N bond length for the former is likely to be shorter than the latter,[8] giving a higher peak wave number for the former as expected. The calculated absorption intensities for both bands can be obtained from the generation probabilities for two kinds of SiN bonds estimated using Table I and the values of $A_p(n)$ determined previously, and are shown as a function of x(calc) by the solid curves in Fig. 3. Here, we used the oscillator strength of 6.3×10^{18} cm^{-2} for both 840 and 960 cm^{-1} bands, which has been determined by a comparison between the SiN absorption intensity and the x value estimated from

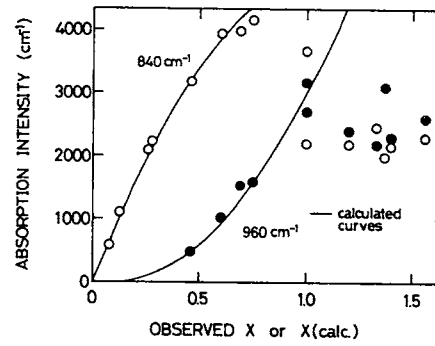

FIG. 3. Integrated absorption intensity of the 840 cm^{-1} (○) and 960 cm^{-1} (●) bands obtained from the SiN asymmetric stretching mode, as a function of the observed N content x. The solid curves as a function of x(calc) are calculated by the random bonding model including SiH and NH bonds.

EPMA.[10] Up to around $x = 0.9$, the observed values for both bands agree well with the corresponding calculated curves, but fall off at x above 0.9. The reduction in these absorptions might be due to an increase in the oscillator strength with x above 0.9.

We are indebted to Professor T. Shimizu for stimulating discussions.

[1] M. J. Powell, B. C. Easton, and O. F. Hill, Appl. Phys. Lett. **38**, 794 (1981).
[2] V. Šmid, N. M. Dung, L. Štourac, and K. Jurek, J. Non-Cryst. Solids **70**, 1 (1985).
[3] R. A. Street and C. C. Tsai, Appl. Phys. Lett. **48**, 1672 (1986).
[4] A. K. Sinha, H. J. Levinstein, T. E. Smith, G. Quintana, and S. E. Haszko, J. Electrochem. Soc. **125**, 601 (1978).
[5] R. Kärcher, L. Ley, and R. L. Johnson, Phys. Rev. B **30**, 1896 (1984).
[6] S. Hasegawa, T. Tsukao, and P. C. Zalm, J. Appl. Phys. **61**, 2916 (1987).
[7] A. Morimoto, Y. Tsujimura, M. Kumeda, and T. Shimizu, Jpn. J. Appl. Phys. **24**, 1394 (1985).
[8] D. V. Tsu, G. Lucovsky, and N. J. Mantini, Phys. Rev. B **33**, 7069 (1986).
[9] S. Hasegawa, M. Matuura, H. Anbutsu, and Y. Kurata, Philos. Mag. B **56**, 633 (1987).
[10] S. Hasegawa, H. Anbutsu, and Y. Kurata, Philos. Mag. B **59**, 365 (1989).
[11] S. Hasegawa, S. Narikawa, and Y. Kurata, Philos. Mag. B **48**, 431 (1983).
[12] H. Shanks, C. J. Fang, L. Ley, M. Cardona, F. J. Demond, and S. Kalbitzer, Phys. Status. Solidi B **100**, 43 (1980).
[13] W. A. Lanford and M. J. Rand, J. Appl. Phys. **49**, 2473 (1978).
[14] W. R. Knolle and J. W. Osenbach, J. Appl. Phys. **58**, 1248 (1985).
[15] G. Lucovsky, Solid State Commun. **29**, 571 (1979).
[16] E. Parthe, *Crystal Chemistry of Tetrahedral Structures* (Gordon and Breach, New York, 1964), p. 73.
[17] D. Della Sala, C. Coluzza, G. Fortunato, and F. Evangelisti, J. Non-Cryst. Solids **77/78**, 933 (1985).

Faculty of Technology, Kanazawa University[1])

Study on Dislocation–Impurity Interaction by the Blaha Effect

By

T. OHGAKU and N. TAKEUCHI

Strain rate cycling test is carried out during the Blaha effect measurement for KCl single crystals doped with Br^- and I^- at several concentrations. It is found that the dislocation velocity–stress exponent, m^*, is independent of the impurity concentration but the effective stress, σ_p, due to impurity increases with increasing impurity concentration. Therefore, m^* represents an interaction between a dislocation and an impurity. The strain rate cycling test during the Blaha effect measurement can give the effective stress due to an impurity, separated from other ones. Further, it gives information for a kind of weak obstacle during plastic deformation.

Der zyklische Belastungstest (Änderung der Verformungsgeschwindigkeit) wird während der Messung des Blaha-Effektes an KCl-Einkristallen, dotiert mit Br^- und I^- in verschiedenen Konzentrationen, durchgeführt. Es wird gefunden, daß der Versetzungsgeschwindigkeits–Spannungs-Exponent, m^*, unabhängig von der Konzentration der Verunreinigung ist, jedoch die effektive Spannung, σ_p, infolge der Verunreinigung mit zunehmender Verunreinigungskonzentration zunimmt. Deshalb stellt m^* eine Wechselwirkung zwischen einer Versetzung und einer Verunreinigung dar. Der zyklische Belastungstest während der Messungen des Blaha-Effektes kann die von den Verunreinigungen verursachten effektiven Spannungen getrennt von anderen Spannungen angeben. Weiterhin gibt er Informationen über die Art des schwachen Hindernisses während der plastischen Verformung.

1. Introduction

It is well known that the average velocity, v, of dislocations is empirically expressed as a power function of effective stress, σ_e [1],

$$v = B\sigma_e^{m^*},$$

where B is a constant and m^* the dislocation velocity–stress exponent. A large number of studies have been performed to determine m^* or the effective stress by an indirect method on the basis of the above relation [2 to 5]. However, Srinivasan et al. [6] have reported that m^*-determinations in general have doubtful significance since indirect methods of determination of m^* do not yield a unique value in either MgO or LiF. On the other hand, Gutmanas et al. [7] have reported that m^* decreases rapidly with decreasing concentration of the divalent impurity. Further, m^* has been expressed by a formula which is derived from interaction between a dislocation and impurities [8, 9].

Interaction between a dislocation and impurities has been investigated by solution hardening experiments [10 to 14], direct observation of the dislocation [15 to 17], and internal friction measurement [18 to 22]. Further, dislocation motion in a crystal field containing a number of obstacles has been studied by simulation methods [23 to 25] and a theoretical analysis has been developed [26 to 30]. However, most of the investigations

[1]) Kodatsuno 2-40-20, Kanazawa 920, Japan.

Reprinted from Phys. Stat. Sol. (a), Vol.118,No.153,pp.153~159 (1990.3)